Validation, Measurement and Investigation of Membrane Residue Curves

Naadhira Seedat

Master of Science in Engineering by Research only:

A dissertation submitted to the Faculty of Engineering and the Built Environment,
University of the Witwatersrand, Johannesburg, South Africa

Johannesburg, 2014

DECLARATION

I hereby declare this dissertation as my own unaided work. It is being submitted for the Degree of Master of Science in Engineering to the University of the Witswatersrand, Johannesburg. It has not been submitted for any degree or examination in any other University

……

(Signature of Candidate)

…… day of …… year ….....

ABSTRACT

Membrane residue curve maps (M-RCMs) are a useful graphical tool developed by Peters, M.; Kauchali, S.; Hildebrandt, D.; Glasser, D. (2006) to better understand and design membrane separations. The maps, initially developed theoretically, track the compositional change of the retentate with time during batch permeation.

This dissertation looks at the modification and operation of an experimental apparatus for the measurement and hence existence of M-RCMs. For demonstration purposes, gas separation was chosen for the basis of the membrane separation system. The gas mixture consisted of syngas with carbon dioxide as an impurity through a polyethylene membrane.

The theoretical transport of gases moving through the membrane was developed by a solution-diffusion model that fitted the experimental system adequately. The experimental setup was successfully operated as the results obtained correlate to the theoretical models chosen. In addition, the experimental apparatus can be used for the validation of M-RCMs for any type of membrane and mixture of gases.

DEDICATION

I dedicate this work to my dear parents, Dr AK Seedat and Anisha Seedat. The creator has blessed me by granting me the both of you as my parents. I love you both dearly.

ACKNOWLEDGMENT

In the name of Allah, the most gracious and ever merciful.

First and above all, I praise and I am immensely grateful to ALLAH, the Almighty for showering his mercy and blessings on me and giving me the strength and capabilities to complete my dissertation.

There are many people I am truly grateful to for their help and without whom it would not have been possible for me to complete this dissertation. Dr Mark Peters, my supervisor and mentor who has guided me in completing this dissertation and publication. Thank you so much for the encouragement, advice and support.

I am extremely fortunate to have been able to turn to two of the most accomplished individuals I have ever met, Prof David Glasser and Prof Diane Hildebrandt. I am truly blessed that I was able to have the advice of the two best Chemical Engineers in the world. I thank you for all of your precious time and for all the knowledge you have imparted on me.

Pretesh Parag, one of my closest friends who was always there to help and nudge me to carry on in my darkest and most frustrating moments of experimental work. My dearest friend, Nikita Ranchod for helping me in the lab when required as well as the unlimited emotional support during my undergrad and masters degrees, Thank you.

My gratitude to Dr Daniele Beneke, Emmanuel Kasese, Neil Stacey, Ari Hadjitheodorou, Edward Bono and the entire Separations team for weekly advice, ideas and discussions that gave me a different perspective on the work at hand. My friend and colleague

Emmanuel Kasese, Thank you buddy for all the support, encouragement and for always being there when I needed someone to speak to.

The University of Witswatersrand for financial support and academic platform to extend my knowledge. Thank you to everyone in the School of Chemical and Metallurgical Engineering and COMPS for their support and help daily.

My loving family, Mum, Dad, Tasneem and Sameera Seedat. Thank you for the love, support and patience during my entire schooling career. God has blessed me by having you all in my life. Last but not the least I am grateful to My Loving Husband, Mohamed Riyaadh Ismail for the endless love, support and encouragement to carry on and reminder to have faith in our creator, ALLAH and all will work out in our favour.

Table of Contents

DECLARATION ii
DEDICATION iv
ACKNOWLEDGMENT v
List of Figures ix
List of Tables xi
Nomenclature xii
Chapter 1 1
Synopsis 1
1.1 Introduction 1
1.2 Dissertation Overview 4
Chapter 2 7
Literature Review 7
Chapter 3 14
Theory 14
3.1 Derivation of M-RCM 14
3.1.1 Mass balance 15
3.1.2 Permeation Model 17
3.1.3 Permeability Coefficients 19
3.2 Properties of M-RCMs 20
3.2.1 Stationary Points 20
2.2.2 Membrane Vector Field 21
2.3 Theoretical Curves 22
Chapter 4 25
Research Procedure 25
4.1 Apparatus and materials 25
4.2 Experimental Procedure and Conditions 33
4.3 Sample Analysis 35
Chapter 5 37
Experimental Results and Discussion 37
5.1 Experimental Behaviour 40
5.2 Stationary points behavioural results and discussion 45

5.2.1 Unstable Node behaviour 45
5.2.2 Stable Node behaviour 47
5.2.3 Saddle Node behaviour 50
5.3 Experimental error analysis 53
Chapter 6 55
Conclusion 55
Recommendation 56
References 58
Appendix A: Derivation of the Residue Curve Equation 61
Appendix B: Experimental Results 63

List of Figures

Figure 3.1: Batch membrane gas system with retentate, R, at a higher pressure and permeate, P. 15

Figure 3.2: Membrane residue curve map for an ideal system A-B-C system with αABM=3, αCBM=1.5 and r = 10 (Peters et al., 2006). 21

Figure 3.3: Ideal M-RCM of hydrogen (A), carbon monoxide (B) and carbon dioxide (C) system with $\alpha ABM = 31$ and $\alpha BCM = 60$. 23

Figure 4.1: Experimental Set- up of the apparatus (refer to Table 4-1 for key). 27

Figure 4.2: Schematic depiction of the PPC membrane support wrapped in the polyethylene membrane. 29

Figure 4.3: Plastic container bags used to hold gas mixture. 31

Figure 4.4: Vacuum pump and associated control mechanism. 32

Figure 5.1: Two experimental runs on a single theoretical membrane curve. 39

Figure 5.2: Residue curve map depicting the theoretical and experimental data for the four regions under analysis. The direction of the data progression over a run is from the feed point (for a run) moving towards pure C. 41

Figure 5.3: Experimental data for multiple different feeds on a single theoretical residue curve. 44

Figure 5.4: Experimental data behaviour in the vicinity of the unstable (H_2) stationary point. 46

Figure 5.5: Behaviour of the experimental data in the vicinity of the stable (CO_2) stationary point. 48

Figure 5.6: Zoomed in representation of experimental and theoretical data in the vicinity of the stable node, carbon dioxide. The order of the samples were taken are indicated numerical. 49

Figure 5.7: Experimental data behaviour for different feed points on the saddle node (CO). 51

Figure 5.8: Zoomed in representation of the experimental data for the saddle node depicted in Figure 5.7. 52

List of Tables

Table 4-1: Labelling Key for Figure 4.1 28

Table B-1: Unstable Stationary Point (H_2) Experimental Data 63

Table B-2: Stable Stationary Point (CO_2) Experimental Data 63

Table B-3: Saddle Point (CO) Experimental Data 64

Table B-4: Middle Region Curve Experimental Data 66

Nomenclature

Symbols

A = effective membrane surface area [m]

A = hydrogen

B = carbon monoxide

C = carbon dioxide

J_i = flux o f component i through membrane [mol/ (s.m^2)]

l = membrane thickness [m]

n = number of components

$\dot{P}$ = permeate rate through membrane [mol/s]

P'_i= permeability coefficient of component i [(mol.m)/ (s.m^2.Pa)]

P_p = permeate pressure [Pa]

R_r = retentate pressure [Pa]

R = retentate holdup [mol]

Ro = retentate holdup at t=0 [mol]

Rt = retentate holdup at time t [mol]

t = time [s]

x = retentate molar composition

$x_0 =$ retentate feed molar composition

$y =$ permeate molar composition

Greek letters

$\alpha^M{}_{ij}$ = ratio of membrane permeabilities (selectivity)

$\tau =$dimensionless time

Subscripts

i = reference to component i

j = reference to component j

P = reference to permeate

R = reference to retentate

Superscripts

M = refers to membrane

Abbreviations

MBT = mass balance triangle

M-RCM = membrane residue curve map

PVC = Polyvinyl Chloride

Chapter 1

Synopsis

1.1 Introduction

Separation processes are an essential and integral part of all chemical industrial processes. Almost every process requires efficient separation of products from reactants and impurities as well as other applications. There are different methods of separation used in industry such as distillation, absorbtion, liquid-liquid extraction as well as membrane separations. Membrane separations have in recent times become a successful alternative method for separation of liquid and gaseous mixtures (Peters, et al., 2006). Membrane separation processes have been proven to be a more economical and efficient alternative to distillation in certain applications such as gas separation (Peters, et al., 2006).

The conventional method of analysing membrane systems was to consider the particular feed and from there determine what possible permeates could be achieved. This method is not robust and hence a need for an efficient graphical method was required. Residue curve maps are a graphical tool, originally used in distillation design, and have produced numerous forms of short-hand design methods in the understanding and designing of complex distillation systems

(Doherty & Malone, 2001; Fien & Liu, 1994). Although membrane separations are physically different to operate and design than distillation systems, residue curve maps for membrane systems were developed by Peters et al., (2006) to better understand and design membrane systems. While Peters et al., (2006) developed the theoretical groundwork for membrane residue curve maps (M-RCMs) and later developed and showed their applications to batch and continuous process as well as hybrid systems (Peters, et al., 2008), the main aim of this work is to measure and evaluate an experimental technique for generating M-RCMs.

Membrane separation technology is a rapidly growing development. Membrane systems have proven to require less energy and lower capital costs hence reducing operating and start-up costs (Rautenbach & Albrecht, 1989). In industry, membrane systems are easily installed, operated and require limited space (in comparison to other separation processes). Membrane separation is also an equilibrium-independent process which can reach higher yields than conventional separations processes (Peters, et al., 2006). Membrane gas separation, for example, is gradually becoming a more important separation technology in areas such as air separation, hydrogen recovery and natural gas purification (Pettersen & Lien, 1995). In this regard, membrane separation is a conceptually simple process. However, there are many design decisions with respect to selection of operating conditions, module configurations and suitable membrane materials that need to be made (Pettersen & Lien, 1995).

M-RCMs plot the change in the retentate composition with time in a batch still (Peters, et al., 2006). M-RCMs are a graphical technique that are derived from

mass balances constraints and incorporate the appropriate models in order to interpret, analyze and design membrane separation processes efficiently (Peters, et al., 2006). Initially the use of residue curve maps was constrained by the understanding of equilibrium-based processes but since the construction of the maps are based on material balances that enables the understanding of equilibrium and non-equilibrium based systems that can be extended to understanding kinetic systems (Peters, et al., 2006). Hence membrane residue curve like distillation residue curves (D-RCM) are useful tools used in industry to design and analyze the respective separation system to be implemented in industrial processes. M-RCMs not only introduce a novel graphical method of designing membrane systems, but also provide insight into optimization and attainability.

This work is focused on validating and experimentally measuring residue curve maps for membrane separations developed by Peters et al., (2006). For reasons of simplification, the validation of M-RCM's were done using a non-reactive experimental system. Membrane residue curves were constructed on the basis of experimental data and its validity to membrane separations were analyzed. The validation of membrane residue curves is conducted on gas separation systems but this confirmation can be implied to other forms of membrane systems. The gas separation involves the diffusion of a gaseous batch feed (retentate) consisting of synthesis gas (carbon monoxide and hydrogen) and an impurity of carbon dioxide, at a high pressure; through a simple polyethylene membrane into a low pressure permeate side.

Through the measurement of the M-RCMs experimentally, it further validates the use and effectiveness of M-RCMs in designing and analyzing membrane separations. In addition, if separation processes are able to be synthesised for the above system it will be shown that a simple and inexpensive polyethylene membrane would be sufficient for industrial separations. This would provide an alternative view on designing membrane separations instead of designing expensive membranes, rather use membrane residue curves and simple membranes to achieve the same results economically.

1.2 Dissertation Overview

Parts of the body of the work of this dissertation have been presented at the 2012 SAIChE conference in Drakensburg, South Africa.

The work contained in this dissertation has been published in an internationally-recognized peer-reviewed journal. The publication reference is:

> Seedat, N., Parag, P., Govender, D., Peters, M., Hildebrandt, D., Glasser, D., **2013**. Experimental Measurement of Membrane Residue Curve Maps. *Ind. Eng. Chem. Res.*, *52* (32), pp 11142–11150.

For purposes of ease of reading and dissertation-formatting, the material in each section of the publication has been divided into separate chapters. A summary of each chapter is given below:

.

CHAPTER 2 consists of a literature review on the history of the concepts used to understand gas diffusion through membranes as well as the development of gas separations using membranes and membrane distillation. Additionally it contains existing work done on the theoretical development of M-RCMs and then explains the concept of hybrid membrane-distillation processes.

CHAPTER 3 entails the theoretical work required to better understand M-RCMs. The chapter provides the derivation and properties of M-RCMs such that the theoretical curves for the chosen system of H_2, CO and CO_2 could be generated and understood. Additionally the assumed permeation model and permeability coefficients for the components were stated and explained for the system under investigation.

CHAPTER 4 provides the experimental apparatus and set-up used in order to generate the experimental data required to compare with the theoretical curves generated using theoretical work. This set-up had to allow for the permeation of the gases through a polyethylene membrane under vacuum conditions. A comprehensive experimental procedure as well as the method of analysing samples are stated in this chapter.

CHAPTER 5 illustrates the results of the experimental data obtained from conducting experimental runs through the procedure provided in Chapter 4 and the discussion of the behaviour of the data in relation to the theoretical data generated. The Figures illustrated in this chapter depict the comparison of the

behaviour of the experimental data in relation to the theoretical data generated for a single membrane residue curve in the middle region of the M-RCM and the three stationary points for the system. The system of gases consisted of H_2, CO_2 and CO. The stationary points are: the stable node (CO_2), unstable node (H_2) and saddle node (CO). The behaviour of both the theoretical and experimental curves were found to predict the same behaviour with minimal errors and deviations.

Chapter 2

Literature Review

Separation of gases has found an integral part of industry required in a wide range of applications such as air separation, refinery processes as well syngas purification to name just a few. Membrane separation technology is the most decisive aspect of gas separation technologies hence there has been rapidly growing research and development of industrial application of gas separation membranes (Pandey & Chauhan, 2001). Membrane separations reduce costing in terms of lower energy requirements and lower capital cost in certain applications such as gas separation. Membrane separations are also not limited by vapour-liquid equilibrium which is the case for distillation, liquid-liquid separation and absorption hence achieving higher yields and avoiding the formation of azeotropes (Buchaly et al., 2007).

The first experimentation of the gas transport through membranes began as early as 1829 (Pandey & Chauhan, 2001). Development of membrane for filtration and water purification advanced throughout the 1930s to 1950s (Pandey & Chauhan, 2001). Membrane distillation development first appeared in literature in the late 1960s after which there was decline in research into membrane distillation (El-Bourawi, et al., 2006). The rebirth of research and development as well as major

improvements were made in the field of membrane distillation began in the 1980s when novel membranes and modules with better characteristics became obtainable (El-Bourawi, et al., 2006).

According to Pandey & Chauhan (2001), two fundamental concepts have formed the basis for the understanding of gas-diffusion phenomena. The first concept was developed in 1829 by Thomas Graham, who performed the first recorded experiment on the transport of gases and vapours through a polymeric membrane (Pandey & Chauhan, 2001). In 1866, Graham published concepts for gas permeation based on a 'solution-diffusion mechanism' (Pandey & Chauhan, 2001). Graham defined the permeation process as a sequence of solution, diffusion, and re-evaporation of the diffusing gas (Brubaker & Krammermeyer, 1953). Graham's law of diffusion is defined as 'when two gases interdiffuse at uniform pressure, their fluxes are in the inverse ratio of the square roots of their molecular weights' and the simplified formula is as follows (Mason & Kronstadt, 1967):

$$\frac{Rate_1}{Rate_2} = \sqrt{\frac{M_2}{M_1}}$$

Where:

$Rate_1$= the rate of diffusion of gas 1
$Rate_2$= the rate of diffusion of gas 2
M_1= molar mass of gas 1
M_2= molar mass of gas 2

In 1855, Adolf Fick proposed a quantitative description of material transport through boundary layers (Pandey & Chauhan, 2001). This forms the second fundamental concept in understanding gas-diffusion through membranes. Another important factor that affects the performance of a membrane and hence the gas diffusion through membranes is the physical properties of the gas and membrane (Pandey & Chauhan, 2001). In 1907, Benchold defined the relationship between physical properties such as bubble point, surface tension, pore radius and the membrane performance (Pandey & Chauhan, 2001). In the same work Benchold (1907) derived a technique to prepare nitrocellulose membranes of graded pore-size structures (Pandey & Chauhan, 2001). In 1933 Karplus modified the method for preparing nitrocellulose membranes and resulted in the preparation of microporous collodion membranes which became commercially available in the 1930s (Pandey & Chauhan, 2001).

Over the next 20 years, there was further development in the field of membrane generation, other polymers such as cellulose acetate was tried in microfiltration membranes (Pandey & Chauhan, 2001). In the 1940s these membranes were widespread used in the filtration of drinking water (Pandey & Chauhan, 2001). By the 1960s there was a vast development in membrane technology and sufficient knowledge was available on the relationship between the structure and function in gas separation membranes (Pandey & Chauhan, 2001). Although these membranes were plagued with various problems such as unreliability, they were costly and non-selective hence producing low fluxes thus their use in industry was restricted (Pandey & Chauhan, 2001). Through the Loub-Sourirajan invention of

the high-flux asymmetric reverse osmosis membranes (RO), membranes began to find their place in industry in the field of water purification (Pandey & Chauhan, 2001). It was only in the late 1970s that membranes proved to be economically competitive in certain industrial applications for gas separation such as the removal of hydrogen form ammonia product streams and Cynara and Separax company used membranes for the separation of carbon dioxide (Pandey & Chauhan, 2001).

During the 1980s there was rapid development and research in the field of membrane science and technology through the development of synthetic membranes (Pandey & Chauhan, 2001). 'A synthetic membrane is a thin barrier between two phases through which differential transport can occur under a variety of driving forces including pressure, concentration and electrical potential across the membrane'. Since this dissertation is focused on gas separation pressure difference is the driving force that will accommodate the permeation of gases through the membrane used. Additionally membrane gas separation emerged in industry on a large scale in the 1980s (Pandey & Chauhan, 2001). This period proved imperative in the field of membranology as vast development was made in this field with respect to improvement in membrane formation processes, chemical and physical properties, configurations and applications (Pandey & Chauhan, 2001).

Membrane distillation was introduced in the late 1960s and the development of membrane distillation accelerated in the 1980s with the growth of membrane

engineering (El-Bourawi, et al., 2006). Membrane distillation claims to be an attractive separation process as membrane distillation is cost effective with respect to be able to function using low grade waste and alternative energy (El-Bourawi, et al., 2006). Due to this fact membrane distillation has ignited a vast amount of interest and research, although from a commercial stand point membrane distillation has not yet been implemented into industry due to various reasons (El-Bourawi, et al., 2006). The major reasons include membrane and module design, membrane pore wetting, low permeate flow rate and flux decay as well as uncertain energetic and economic costs (El-Bourawi, et al., 2006).

The development of membrane separation has grown to be a well defined technology since the development in the research of membranology. Many publications propose that membrane separation could possibly replace conventional distillation (Hinchliffe and Porter, 2000). Most experimental research show advantages in different forms of proposed configurations for membrane separation but no valid methods are available to understand a trend in design methodology for membrane technology. The conventional method of analysing membrane systems was to consider the particular feed and from there determine what possible permeates could be achieved. This method is not robust and hence a need for an efficient graphical method was required. Residue curve maps are a graphical tool, originally used in distillation design, and have produced numerous forms of short-hand design methods in the understanding and designing of complex distillation systems (Doherty & Malone, 2001; Fien & Liu, 1994). Although membrane separations are physically different to operate and design

than distillation systems, residue curve maps for membrane systems were developed by Peters et al., (2006) to better understand and design membrane systems.

Another important need for the development of a graphical method is the need to design and synthesise hybrid distillation-membrane configurations (Peters et al., 2008). Over the years, in the chemical and process industry hybrid configurations has gained increasing importance and focus has been shifted to the development and application of such processes (Buchaly et al., 2007). These integrated systems incorporate the characteristics of the different technologies and exploit these characteristics in an efficient manner thus producing synergetic effects (Pettersen & Lien, 1995; Buchaly et al., 2007). Through the improvements gained by the synergetic effects of these processes the benefits are evident in the reduction of equipment and plant size as well as improved process efficiencies hence yielding a better process economy (Buchaly et al., 2007). In addition hybrid configurations have become increasingly attractive due to the reduction in capital and operational costs as well as the potential energy savings (Stephan et al., 1994). According to Pettersen et al., (1996) substantial work has not been published on the systematic design methods of hybrid distillation-membrane configurations.

With the establishment of M-RCMs by Peters et al., (2006) not only does the maps serve as a method of understanding and designing membrane separations but also a novel graphical technique for designing hybrid configurations. Peters et al., (2008) looks at the design of a hybrid configuration M-RCMs and D-RCMs.

Peters et al., (2006) formulated a graphical technique that incorporates mass balances as well as the appropriate permeation models in order to interpret, design and analyse membrane separations in an efficient and useful manner. This graphical technique developed is known as membrane residue curve maps (M-RCMs). M-RCMs track the change in retentate composition with time in a batch still (Peters et al., 2006). Since M-RCMs are derived from a combination of mass balances, they are applicable to equilibrium based processes as well as kinetically based processes such as reactive distillation and membrane separation processes (Peters et al., 2006).

Chapter 3

Theory

3.1 Derivation of M-RCM

In order to generate M-RCMs, a batch system of gases enclosed by an appropriate membrane as in Figure 3.1 is considered. A constant pressure difference across each side of the membrane is assumed. The pressure difference is constant for a specific experimental run but differs from one run to the next (refer to Chapter 4 and 5). A higher pressure occurs on the feed-side (retentate, R), causing the gases to permeate through the membrane and move into the permeate side ($\dot{P}$) of the system. The permeate is removed from the system as it is formed, allowing separation to continue until all the high pressure fluid has permeated through the membrane.

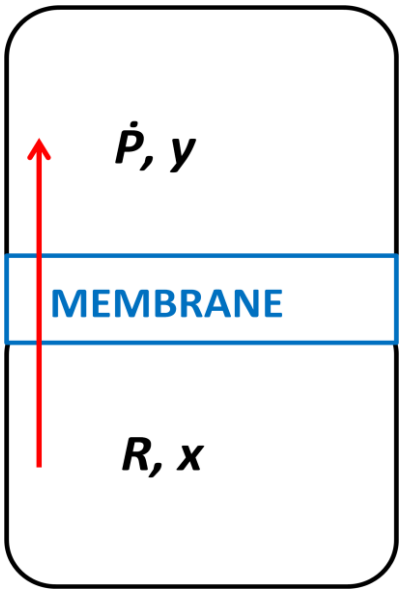

Figure 3.1: Batch membrane gas system with retentate, R, at a higher pressure and permeate, Ṗ.

3.1.1 Mass balance

The system in Figure 3.1 is based on the assumptions that the gas components are non-reactive with each other, nor with the material of the membrane and system. Performing an instantaneous overall mass balance on Figure 3.1 produces (Peters et al., 2006):

$$-\frac{dR}{dt} = \dot{P} \qquad (3.1)$$

where R refers to the amount of retentate [mol], $\dot{P}$ refers to the amount permeated through the membrane per unit time [mol/s] and t refers to time [s].

Performing a component balance on the system, with respect to component i, further relates the permeate flow to the change in retentate.

$$\dot{P}y_i = -\frac{d(Rx_i)}{dt} \qquad (3.2)$$

$$\dot{P}y_i + x_i\frac{dR}{dt} + R\frac{dx_i}{dt} = 0 \qquad (3.3)$$

Equation (3.2) refers to a component balance over the system where *x* and *y* refer to the compositions of the retentate and permeate respectively, with respect to component *i*. The algebraic simplification of Equation (3.2) is represented by Equation (3.3).

The combination of Equation (3.1) and (3.3) results in the isolation of the retentate and is represented by ordinary differential equations:

$$\frac{dx_i}{d\tau} = (x_i - y_i)\,, i = 1{,}2 \ldots n-1 \qquad (3.4)$$

Where *n* refers to the number of components within the system and τ is dimensionless variable with respect to time and is equated to *–ln(Ro/Rt)* where *Ro* and *Rt* refers to the retentate initially and at time *t* respectively. Equation (3.4) records the retentate composition with respect to time for a given set of boundary conditions (feed compositions, x_0). A full derivation of the Equation (3.4) can be found in Appendix A. Hence a series of curves will be produced for different feed points and will result in a membrane residue curve map (M-RCM). The derivation of Equation (3.4) was first done on a liquid system by Peters et al., (2006) but this equation is also applicable to gaseous systems.

By definition, a membrane residue curve map (M-RCM) is a plot of the change in composition of the retentate in a batch still over time (Peters et al., 2006). This definition is mathematically described by the derived Equation (3.4). It should also be noted Equation (3.4) is independent of the permeate removal rate, $\dot{P}$ and only dependent on the change in composition.

3.1.2 Permeation Model

In order to solve the differential equations in Equation (3.4) a relationship between the retentate (x_i) and permeate (y_i) compositions needs to be defined by a non-equilibrated permeation model (Peters et al., 2006). Many experimental models exist in describing permeation. Peters et al, 2006 uses a fundamental thermodynamic approach using the permeation model described by Wijmans and Baker, (1995) as depicted in Equation (3.5):

$$J_i = \frac{P'_i(P_r x_i - P_p y_i)}{l} \qquad (3.5)$$

where J_i is the volumetric transport of component i through the membrane [mol/(s.m^2)], P'_i is the permeation coefficient of component i [(mol.m)/(s.m^2.Pa)], l refers to the membrane thickness [m] and P_r and P_p is the total pressure [Pa] of the retentate and permeate respectively. Wijmans and Baker. (1995) Equation (3.5) applies to gas separation only and has been derived from first principals.

The experiment conducted in this dissertation is assumed to be conducted under vacuum conditions resulting in a permeate pressure of zero. This assumption simplifies Equation (3.5) accordingly:

$$J_i = \frac{P'_i P_r x_i}{l} \qquad (3.6)$$

According to Peters et al., (2006) the flux of a component, i is the amount of material that permeates through the membrane per unit time per unit area, this is represented in Equation (3.7):

$$J_i = \frac{\dot{P} y_i}{A} \qquad (3.7)$$

where A refers to the effective membrane surface area [m^2] and $\dot{P}$ is the permeate flow in [mol/s].

By equating Equations (3.6) and (3.7) with respect to component *i* and component *j* and then dividing the expressions by each other, produces a general model that relates the retentate and permeate compositions given in Equation (3.8) (Peters et al., 2006):

$$\frac{y_i}{y_j} = {\alpha_{ij}}^M \frac{(r x_i - y_i)}{(r x_j - y_j)} \qquad (3.8)$$

where ${\alpha_{ij}}^M$ (membrane selectivity) is the permeability coefficient of component *i* with respect to the permeability coefficient of component *j* and r is the ratio of pressures.

In addition if the system is to be operated at vacuum conditions i.e $P_p = 0$. This is mathematically described by Equation (3.9):

$$\frac{y_i}{y_j} = {\alpha_{ij}}^M \frac{x_i}{x_j} \qquad (3.9)$$

Equation (3.9) is sufficient for the solution of Equation (3.4) which is then used for the graphical generation of M-RCMs.

3.1.3 Permeability Coefficients

The permeability of a gas to move through a membrane media is usually a series of correlations that account for system properties and material. A constant relative permeability for each component is assumed for the system of this experiment. This ideal assumption is made for the simplicity of describing the system. The gas system used in this experiment composes of three gases, hydrogen (A), carbon monoxide (B) and carbon dioxide (C). The constant relative permeabilities at 25°C of these components relative to the carbon monoxide flux rate are represented as:

$$\alpha_{AB}{}^{M} = 31 \text{ and } \alpha_{BC}{}^{M} = 60$$

These relative permeabilities are based on mass transfer through a natural rubber membrane and are adapted from Geankoplis (1993) and Michaels & Bixer, (1961). Hydrogen has a large permeability with respect to the other components and will move the fastest through a natural rubber membrane. Carbon dioxide will behave as an intermediate permeater and carbon dioxide will move very slowly through the membrane.

Permeability has a large dependence on partial pressure of the system. The driving force of the system is purely based on the partial pressure of the system; this relation is represented by Equation (3.5). Partial pressure is directly proportion to the concentration of the system.

The concentration of the system continuously changes with time and therefore this will continuously change the partial pressure of the system.

3.2 Properties of M-RCMs

3.2.1 Stationary Points

Stationary points are points of pure components and the composition of a component is equal on both sides of the membrane i.e. $x_i = y_i$ (Peters et al., 2006). Stationary points can be classified into three types namely: stable, unstable and saddle points (Fien and Liu., 1994; Huang et al., 2004). Consider the stationary points in the M-RCM depicted in Figure 3.2 adapted from Peters et al., (2006) for an ideal system of A-B-C. Pure A is the unstable node as it is the fastest permeating component and the curves move away from A as the retentate is rapidly depleted of A. Pure B is the stable node as it is the slowest permeating component hence the retentate becomes richer in B which is seen in the curves moving towards B. Pure C is the saddle node as the curves move towards and then away from C hence causing curvature but does not reach pure C as this is the intermediate permeating component. It should be noted that stationary points also occur at arheotropes, although the system does not exhibit this phenomena (Peters et al., 2006).

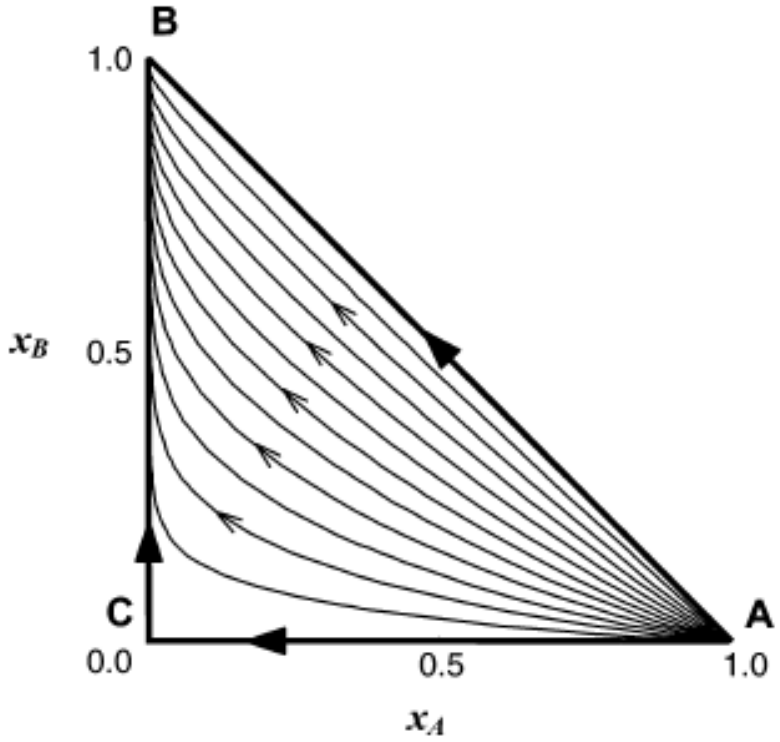

Figure 3.2: Membrane residue curve map for an ideal system A-B-C system with $\alpha_{AB}{}^{M}$=3, $\alpha_{CB}{}^{M}$=1.5 and r = 10 (Peters et al., 2006).

2.2.2 Membrane Vector Field

The set of ordinary differential equations in Equation (3.4) can be reduced to one ODE by defining *x* and *y* as vectors. Therefore Equation (3.4) can be modified into a vector form:

$$\frac{d\vec{x}}{d\tau} = [\vec{x} - \vec{y}] \qquad (3.10)$$

The right-hand side of Equation (3.10) is referred to as a membrane separation vector and is defined as in Equation (3.11), (Peters et al., 2006):

$$\overrightarrow{S^M} = [\vec{x} - \vec{y}] \qquad (3.11)$$

where $\overrightarrow{S^M}$ is the right-hand side of Equation (3.11) in vector form thus, one can define the separation vector as the difference between the permeate and retentate compositions at a specific time which is the degree of separation obtained at any time (Peters et al., 2006). Additionally the separation vector is viewed as tangent to a residue curve map at a retentate composition (Peters et al., 2006). From a tangential point of view, the separation vector can be represented as a function of $\vec{x}$ at any point on the M-RCM.

As with D-RCMs and column profile maps (CPM) which are efficient graphical methods of designing distillation systems with the development of M-RCMs a proficient graphical method is available to synthesise, design and analyse membrane systems as well as hybrid membrane-distillation configurations. Hence the experimental validation and measurement of M-RCMs and synthesising of membrane separations will further establish the usefulness, efficiency and applicability of M-RCMs.

2.3 Theoretical Curves

Figure 3.3 represents a theoretical M-RCM of a hydrogen, carbon monoxide and carbon dioxide system. The construction of the map was conducted by solving Equation (3.4) and (3.9) simultaneously and using the constant relative permeabilities, with respect to natural rubber, as mentioned before. Matlab software program was used in order to solve Equation (3.4) and (3.9) simultaneously to generate the theoretical curves.

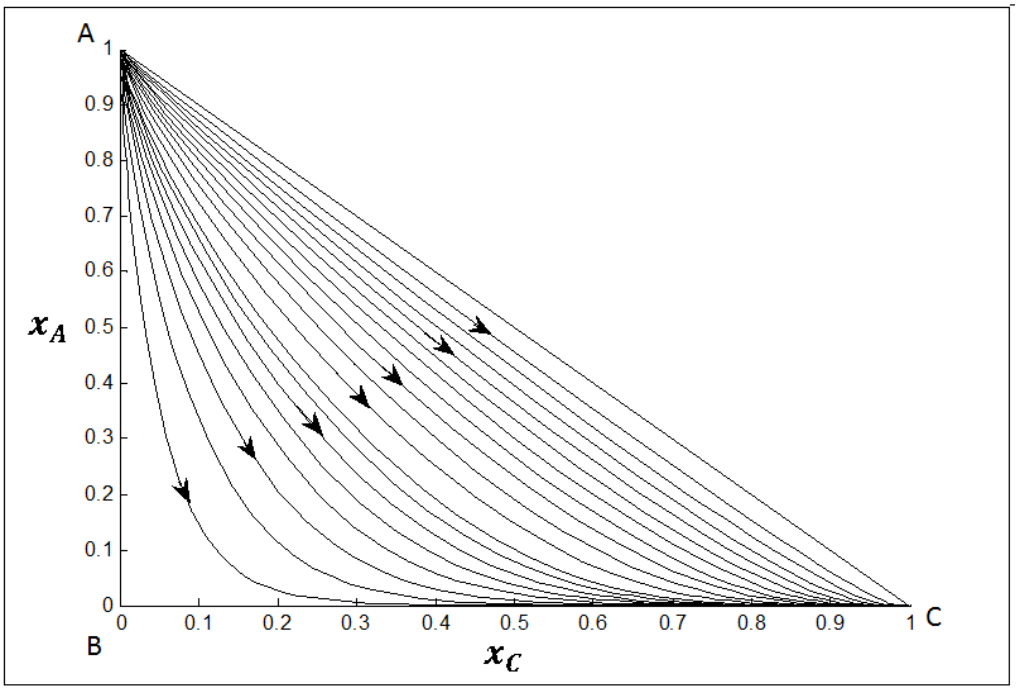

Figure 3.3: Ideal M-RCM of hydrogen (A), carbon monoxide (B) and carbon dioxide (C) system with ${\alpha_{AB}}^{M} = 31$ and ${\alpha_{BC}}^{M} = 60$.

The axes form the boundaries of the mass balance triangle (MBT) which is the region of all physically obtainable compositions in a ternary system.

The curves plotted in the Figure 3.3 within the MBT track the change in retentate (non-permeate) composition with time. The trend in these curves promotes rapid movement from the fastest permeater (A-hydrogen) towards the slowest permeating component (C-carbon dioxide). In other words the curves move from the unstable node (A) to the stable node (C). As the curves move closer to pure carbon monoxide (B), the intermediate component, the trend becomes more curved in nature and never reaches a state of pure carbon monoxide. The nature of the curvature of the curves near the saddle node depict that separation becomes

more difficult at this point as the membrane separation vector tends towards zero. The magnitude of the curvature of the curves near the intermediate component is dependent on the magnitude of the permeability of the component. Larger permeabilities will result in larger curvature since the curves will move closer to the component point before moving away to the fastest permeator.

In conclusion the stationary point of pure hydrogen is the unstable node, the point of pure carbon dioxide is the stable node and the point of pure carbon monoxide is the saddle node.

Chapter 4

Research Procedure

An experimental apparatus was operated such to measure various profiles on a membrane residue curve map (M-RCM). This apparatus operates under batch conditions and the setup has allowed the analysis in the change in retentate composition of a gas mixture. From the tracking of change in the retentate composition it allows the generation of profiles on a M-RCM for different membrane types and different gas mixtures under a host of conditions – this forms part of future research. The current research is the development of the method to generate M-RCMs. The experiments were run isothermally at room temperature of 25°C.

4.1 Apparatus and materials

The experimental apparatus consists of the following equipment:

- A vacuum pump
- A variable voltage controller
- Polyethylene membrane (Glad-wrap) wrapped on a PVC support
- Two plastic bag containers (non-rigid)
- 2 computer fans

- Silicon piping
- Shut off and control valves
- Bubble flowmeter
- Water monometer

Figure 4.1 depicts the experimental apparatus and setup as a whole.

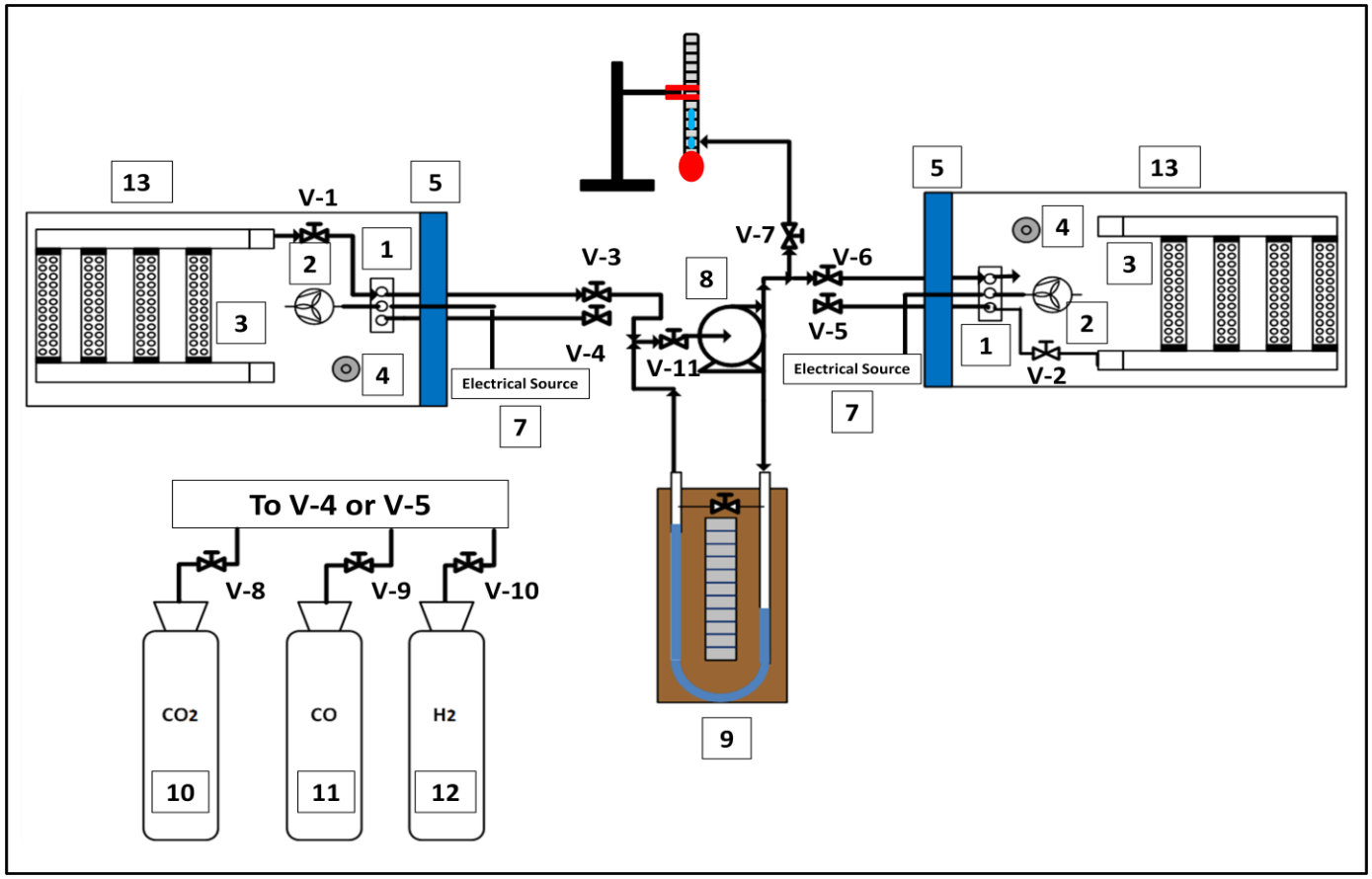

Figure 4.1: Experimental Set- up of the apparatus (refer to Table 4-1 for key).

Table 4-1 serves to annotate the various pieces of apparatus by associating labels to the various circled numbers in Figure 4.1.

Table 4-1: Labelling Key for Figure 4.1

1	Inlet ports for piping and electrical wire.
2	12 volt (D.C.) Brushless fans for agitation.
3	Drilled PVC piping structure (membrane support) and membrane.
4	Septum port for sampling.
5	"Zip-lock" Seal.
6	Bubble Meter.
7	12 Volt D.C. electrical source.
8	Vacuum pump
9	Water Manometer
10	Carbon Dioxide gas cylinder
11	Carbon Monoxide gas cylinder
12	Hydrogen gas cylinder
13	Gas Container (Vacuum plastic bag)
Valves (1,2,3,5,8,9 and 10)	Control Valves
Valves (4,7,6 and 11)	Shut-off Valves

Polyvinyl Chloride (PVC) piping was used to make the membrane support. PVC was used for two very important reasons namely: the strength of the material of construction which is able to withstand under vacuum conditions and the ease with which the relevant piping required could be connected to the support and sealed. PVC piping is generally used in plumbing hence the material, connectors and sealing adhesives were widely and readily available. Holes of a 3mm diameter were drilled into the support to allow for flow of gas through the membrane into the support and hence into the permeate bag. This was achieved by connecting the vacuum pump to the support causing vacuum conditions and hence a pressure difference over the membrane. The pressure difference is the driving force resulting in the gas permeating through the membrane into the support and then into the permeate bag. The area of the membrane support with the drilled holes was covered with membrane and insulation tape was used to attach the membrane to the support. It was essential to ensure that there were no holes on the membrane before using the membrane. The total membrane area available for permeation was $32m^2$.

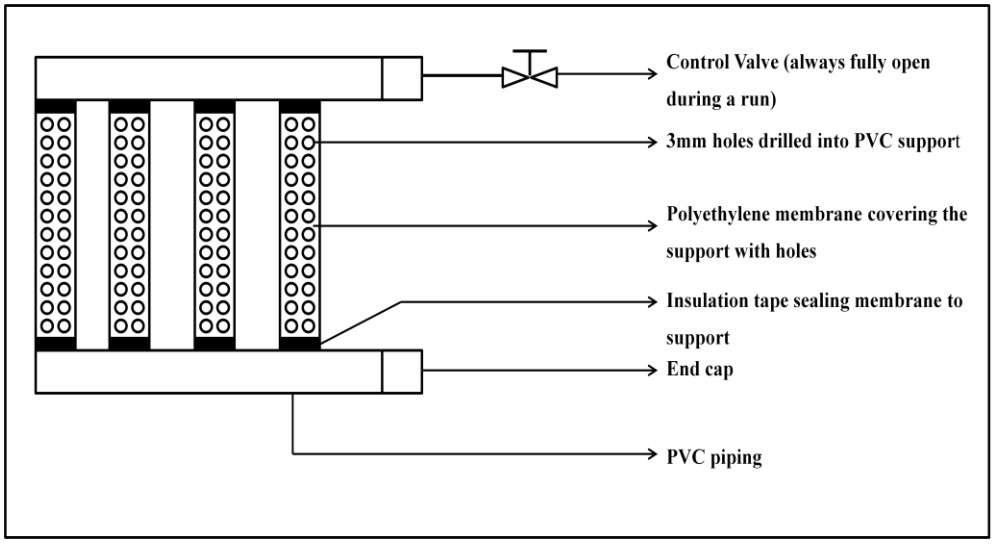

Figure 4.2: Schematic depiction of the PPC membrane support wrapped in the polyethylene membrane.

The plastic containers used look like large storage bags to store clothing and other items. The plastic bags work on the principal of saving storage space and hence a vacuum cleaner is used to evacuate the air in the bag, hence shrinking the contents thus utilising minimal space. In order to serve the above stated purpose the properties of the bags had to be air tight (having a very low or rather negligible permeation rate) and well sealed. By satisfying these properties the bags were well suited for the purpose of the experiment to fill one bag with a fixed volume of gas and using a vacuum pump to transfer the gas through the membrane into the other bag. In addition the bags were also essential as they could be filled with toxic gases without posing a health risk to those exposed to the bags due to leaks or high level of permeation. Furthermore the bags also satisfy the need for there to be negligible permeation of the gas through the walls of the bag, hence ensuring that all the gas moves through the membrane only. This assumption was easily validated, prior to experimentation, by filling each bag with hydrogen and tracking the pressure change over a period of 72 hours. The volume change was also measured. It was found that, after 72 hours, the pressure dropped by 10kPa, and there had been no significant change in the volume of the bags. This is sufficient indication that a negligible amount of gas was lost through the walls of the bag, especially when one considers that the duration of an experimental run is no more than a few (one and two) hours.

The containers had to be further altered for the purposes of the experiment. These alterations include the addition of three ports on each container. For each container, two of the ports were for the purposes of piping and the third for the

electrical wiring required for the computer fans which serves the purpose for agitation of the gas mixture. The agitation was required to obtain a good representative sample as there are large differences in the densities of the gases (hydrogen rises whilst carbon dioxide sinks). There also exists a port on each container which was sealed by means of a rubber septum, this served as the sampling point where a gas syringe could be inserted to obtain samples at a given time. Figure 4.3 shows a single container with the various ports.

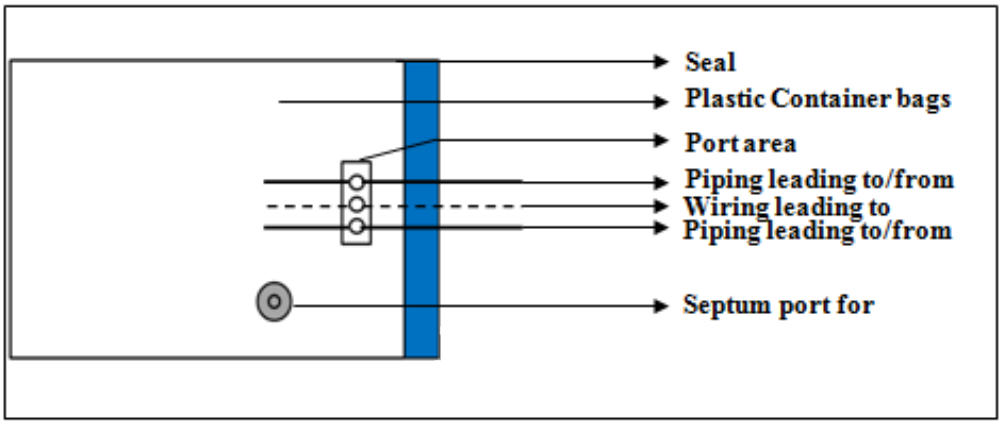

Figure 4.3: Plastic container bags used to hold gas mixture.

The two stage vacuum pump used was controlled by means of a variable voltage controller and a control valve controlling the inlet to the vacuum pump. The variable voltage control allows one to limit the voltage fed to the pump thus directly affecting the shaft power and hence allowing one to control the pump speed. The control valve serves as a fine controller where one could adjust the pressure across the membrane (observed by means of a water manometer). The upstream pressure of the bag when initially filled with gases was a few inches of water gauge above the atmospheric pressure of Johannesburg (approximately 850kPa). While the actual upstream pressure of the system is lowered during a

run, knowledge of it is not necessary to the results. What is important is to maintain a stable difference in pressure (between upstream and downstream) so as to ensure reliable permeation. A manometer reading of about 0.5m water was maintained.

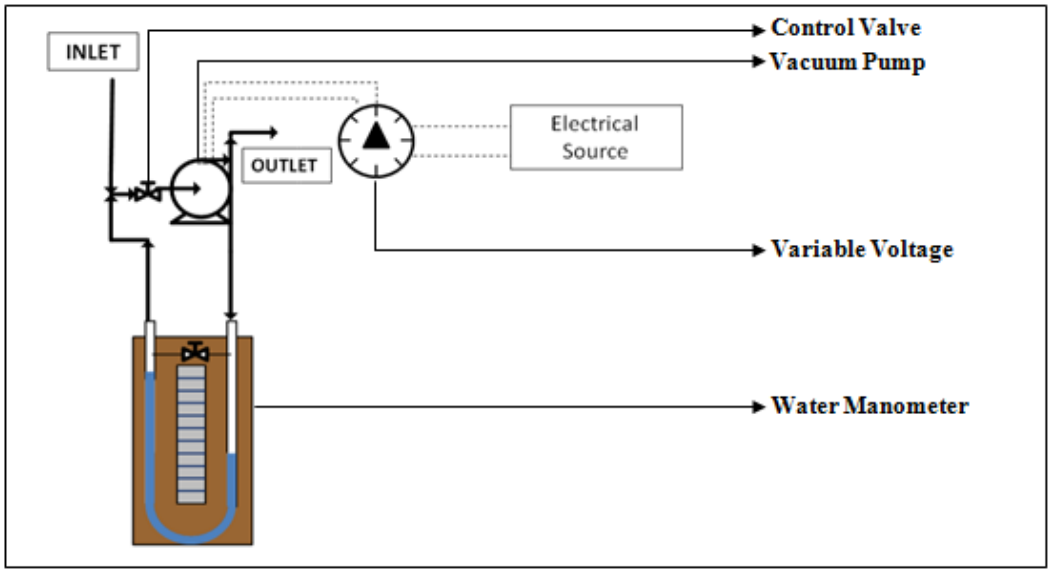

Figure 4.4: Vacuum pump and associated control mechanism.

In order to generate data with a high level of confidence, there were certain aspects of the experimental set-up that had to minimised:

- No punctures in the membrane. These were checked for by using a simple soap-bubble check method.
- No gas losses through the bag walls. This was done (as described earlier) by filling the bags with hydrogen gas and monitoring the change in pressure and volume. The vacuum pump operates as designed.
- Sufficient mixing in the bag is needed to avoid stratification of the gases. This was achieved by the inclusion of the computer fans.

4.2 Experimental Procedure and Conditions

Using the experimental set-up in Figure 4.1 the following experimental procedure was followed to measure and generate membrane residue curves at ambient room conditions:

1. Initially connect V-4 to the vacuum pump and open V-4 and V-11 and switch the pump on to evacuate all the contents of the bag into the vent system of the lab, once evacuated close valves V-4 and V-11. Thereafter evacuate the contents of the second bag by following the same procedure but instead of V-4, V-6 was attached to the pump and opened and closed along with V-11. This was done to ensure all the contents of both bags were evacuated;
2. Once the bags were evacuated and prior to beginning the experimentation the following must be ensured:
    - valves V-1 and V-2 in the bags were opened as they cannot be accessed once experimentation has commenced;
    - the 'zip-lock' seals on both bags were sealed properly and checked there were no leaks using soapy water. If there were leaks soap bubbles would form;
    - the vacuum pump (8) was switched off;
    - all the valves (shut-off and control) were closed besides V-1 and V-2;
3. A known composition of the gas mixture was determined prior to experimentation. In order to obtain this composition, the gas canisters

valves V-8, V-9 and V-10 for the three gases required were connected to a mass flow meter which was then connected to V-4. To add the gases to the desired quantity V-4 was opened and thereafter the canister valves stated above were opened and the mass flow meter switched on to the correct flowrate;

4. Once the gases were filled in the container valves, V-8, V-9 and V-10 were closed and the flow meter switched off;
5. Thereafter valve V-4 was closed;
6. It was ensured there were no leaks in the bags and valves once again using soapy water. If there were leaks soap bubbles will form;
7. Computer fans (2) were switched on for agitation;
8. After a few minutes a sample was taken from the septum port of the retentate bag using a gas syringe and analysed using the gas chromatographer. It takes 15 minutes for the GC to analyse the sample so the run was started 8 minutes into the sample analysis;
9. The run was started as follows:
    - ensured that all valves except V-1, V-2, V-3 and V-6 were closed;
    - the pump was switched on and the control valve (V-11) was opened slightly and thereafter adjusted to ensure the appropriate pressure drop;
10. Five minutes into the run a sample was taken and analysed as soon as the previous sample was complete. As the run proceeds samples were taken every 15 minutes and the pressure drop was monitored and kept at the appropriate pressure drop;

11. Once the run was completed the pump was switched off and thereafter the experiment valves V-3, V-6 and V-11 were closed;
12. The experiment could be run again in the other direction by simply reconnecting the pipe from valve V-3 to valve V-5 and the pipe from valve V-6 to V-4;
13. Thereafter one would adopt steps 6 to 11. The only difference would be the fact that one will be dealing with valves V-5 and V-4 instead of valves V-6 and V-3;
14. Once the experiments were completed the contents of the bags was evacuated in accordance with step 1 into the vent system of the lab.

4.3 Sample Analysis

The samples collected during the experimental procedure were analysed using a gas chromatograph. A Hewlett-Packard 6980A (Agilent 6890) gas chromatographer was used to analyse the samples and contained a packed column consisting of carboxen packing. The following specification applies to the gas chromatograph utilised:

Support Q: 80/100 mesh. Length/OD 2 meters × 1/8 inch. Poropak.

For the purposes of this experiment a Thermal conductivity detector (TCD) was used as it had a universal selectivity (Sheffield Hallam University). This implies that it can be used for a broad spectrum of components.

The carrier gas used was Argon and samples were analysed at an oven temperature of 35°C. In order to analyse the samples the gas chromatographer needed to be calibrated using calibration gas (a gas of known concentration). The calibration was done to an accuracy of 0.5%. Once calibrated, the data obtained is used to calculate relative response factors. By relating the response factors and the peak areas obtained for the components being analysed in the sample the unknown concentration of the gases in the retentate can be determined.

Chapter 5

Experimental Results and Discussion

Membrane Residue curve maps are graphical tools used to design membrane processes as well as hybrid distillation-membrane systems (both membrane and distillation residue curve maps are used). Extensive theoretical work has been done by Peters et al., (2006 and 2008) on M-RCMs whereas this work looks at measuring and hence validating these graphical tools by performing experiments to measure and generate experimental curves.

These experimental curves were measured and plotted using the procedure mentioned in Chapter 4 and are verified with the theoretical curves generated for the system using the theoretical work done by Peters et al., (2006) and assumptions, both mentioned in Chapter 3, in order to soundly validate M-RCMs. Matlab software program was used in order to solve Equation (3.4) and (3.9) simultaneously to generate the theoretical curves. The data obtained is plotted against the theoretical curves corresponding to the same feed point chosen on the theoretical curve such that both sets of data could be compared as in Figures 5.1 to 5.8.

Four regions of the residue curve map were chosen for analysis namely: in the vicinity of the three stationary points and the fourth a single residue curve in the middle region of the map. The stationary points allows for the investigation of the behaviour of the experimental data near the nodes and whether the results obtained correlate to the behaviour predicted by theory. The above regions of the residue map were chosen such that a wide area of the residue curves could be represented, ensuring that the results obtained could be inferred to any point on the map.

A typical run took place over about 1 – 1.5hrs, and using the duration between sampling as discussed in Chapter 4, about five to eight samples were taken per run.

It should be noted that a single experimental run (from filling the bag with "feed" gas to evacuating that gas through the membrane) only produces data over a small range of the entire residue curve within the map refer to Figure 5.1 which has two individual experimental runs. In other words, to cover a wider range of a residue curve, multiple runs were needed. (All runs move in the same direction on the map: from the feed point towards pure C). This can be seen in Figure 5.2, where multiple runs were required to reproduce the curve near pure B and the middle residue curve. The reason for a limited range in data obtained per run is the limited volume of the sample that could be held in the plastic bags. (An analogy could be drawn to a batch boiling to reproduce distillation residue curve maps. A limited amount of data can be obtained from the batch still as all the liquid boils off, and the liquid will need to be replenished in order to extend the data range.

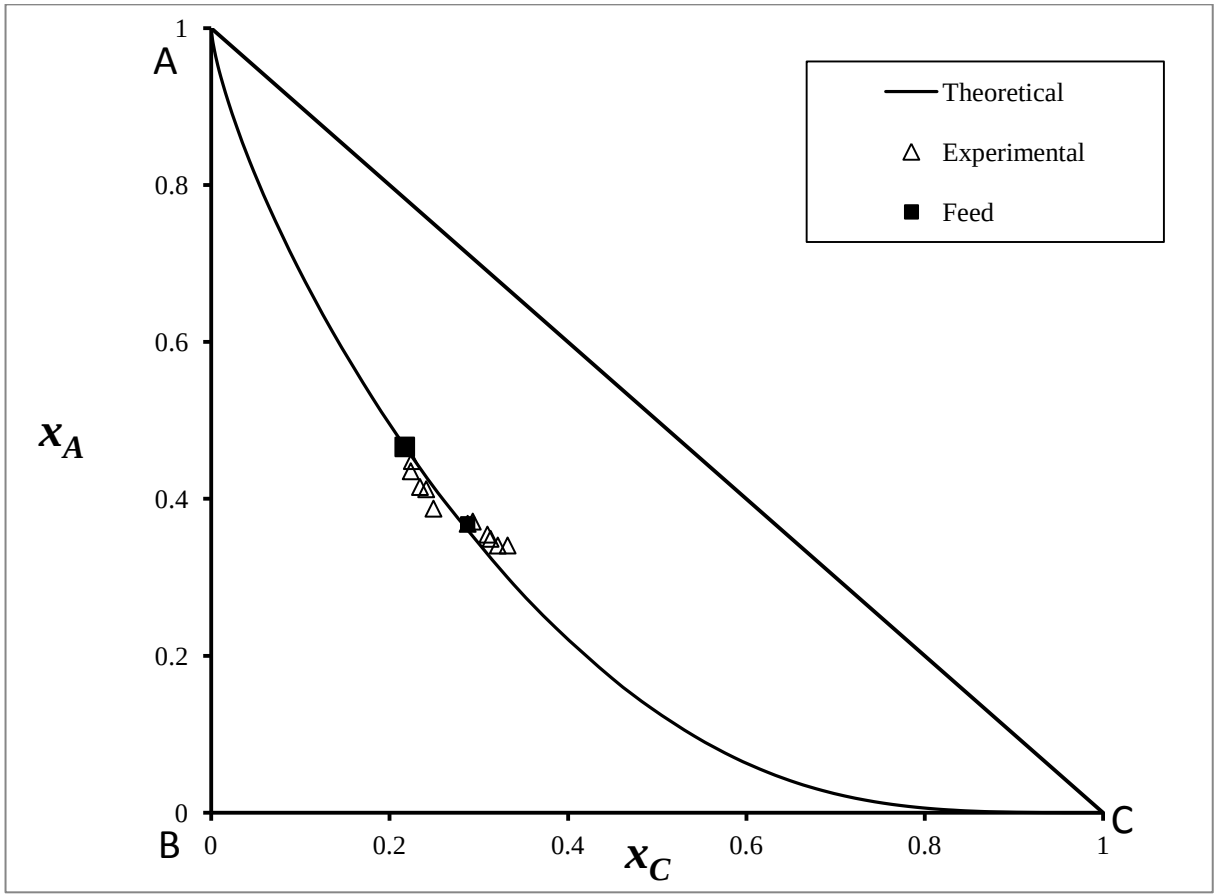

Figure 5.1: Two experimental runs on a single theoretical membrane curve.

5.1 Experimental Behaviour

The theoretical curves and experimental data plotted in Figure 5.2 depicts all four regions that were under investigation. The experimental data plotted in Figure 5.2, progress from the respective feed points towards pure carbon dioxide in all the regions analysed. This behaviour correlates to the theoretical data as the theory predicts that the data moves towards the slowest moving component (the stable node).

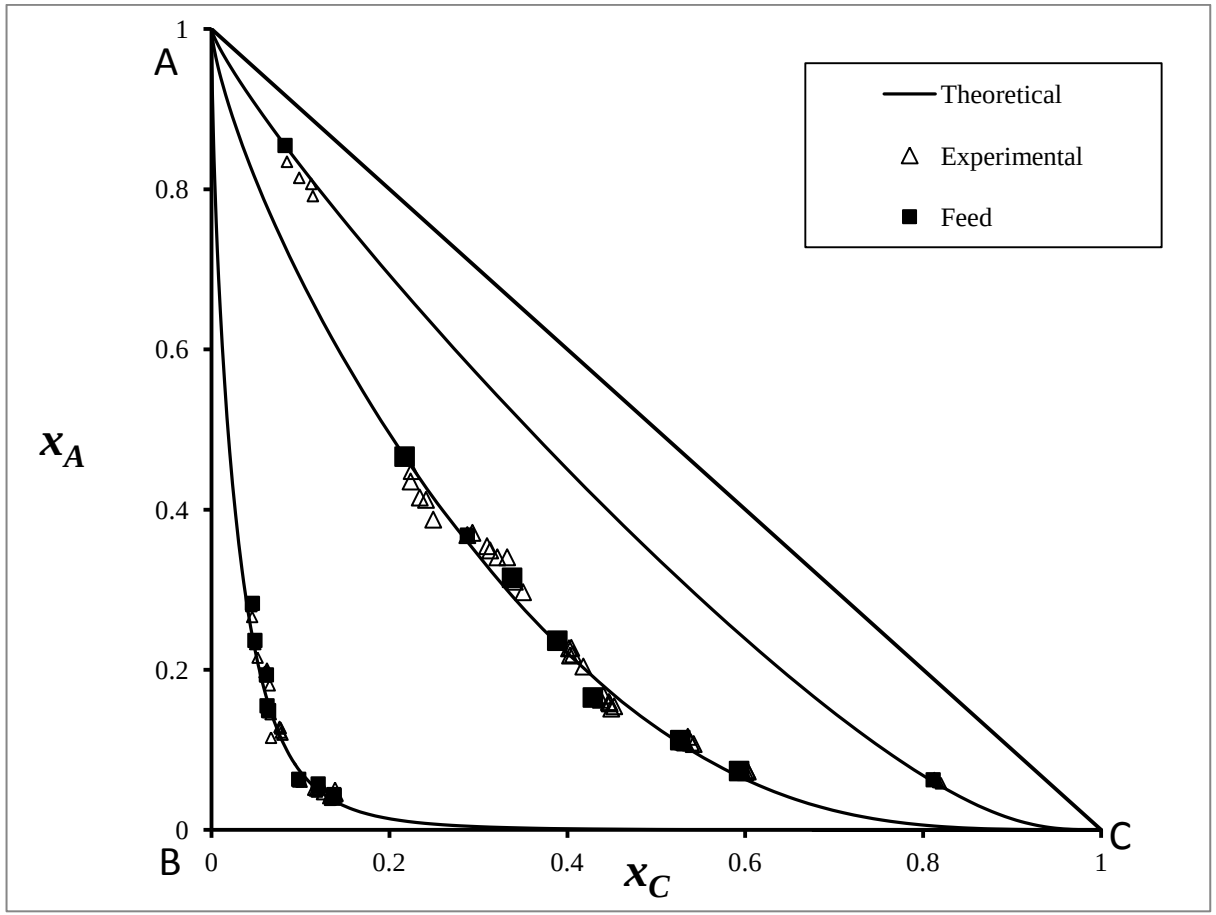

Figure 5.2: Residue curve map depicting the theoretical and experimental data for the four regions under analysis. The direction of the data progression over a run is from the feed point (for a run) moving towards pure C.

Majority of the data obtained correlated to the theoretical data with minimal deviations. The largest deviations of experimental data points from theoretical data in all regions occurred at the last experimental point for each run. These deviations are attributed to the near-vacuum conditions that occur towards the end of the experimental run, once most of the gas material had permeated through the membrane. The near-vacuum condition, formed by the use of the vacuum pump, inhibited a high accuracy result since the sample taken may not be a true reflection of the retentate under this state.

It is interesting to note the behaviour of the middle residue curve in Figure 5.3. Closer inspection of this particular curve reveals that the intermediate component, namely carbon monoxide, labelled B, does not exhibit any drastic change in composition during an experimental run. This can be deduced from the linear and parallel nature of the data relative to the intermediate diagonal axis. In other words, if one were to draw a straight line through these data points (on the middle profile), parallel to the diagonal axis of the MBT, it will be noticed that the data points agree quite well with this line – this indicates that there is no change in carbon monoxide composition with time. Thus, although there is a change in retentate composition with time, it is apparent that this change, for the most part, only occurs due to the other two species, namely hydrogen and carbon dioxide.

Considering the permeability factors of each of the components, it is clear that hydrogen is the fastest permeating species. It can thus be deducted that since the retentate composition of hydrogen is decreasing, and that of carbon monoxide is

constant, the net effect is that the retentate becomes continually richer in carbon dioxide. It is important to note that the magnitude of the carbon monoxide permeability is within a sufficient range from each of the other components and therefore does not change drastically under the non-ideal conditions.

As stated before a single feed point produces a small range of data on the residue curve hence it was recommended to choose the successive feed point to be the preceding run's last data point. Due to inaccuracies in the mass flow meter a feed point close to the chosen point on the same residue could be obtained. Therefore the data obtained is a representation of the behaviour down the profile for feed points on the curve. It can be seen in Figure 5.2 and Figure 5.3 that the trend of each feed point behaves the same, and that is the experimental data move towards pure carbon dioxide, stable node, with respect to time.

It is also important to note that the range of data decreases down the curve per a constant volume of feed. This result is due to the expected behaviour around pure carbon dioxide. This phenomenon is explained later in this chapter.

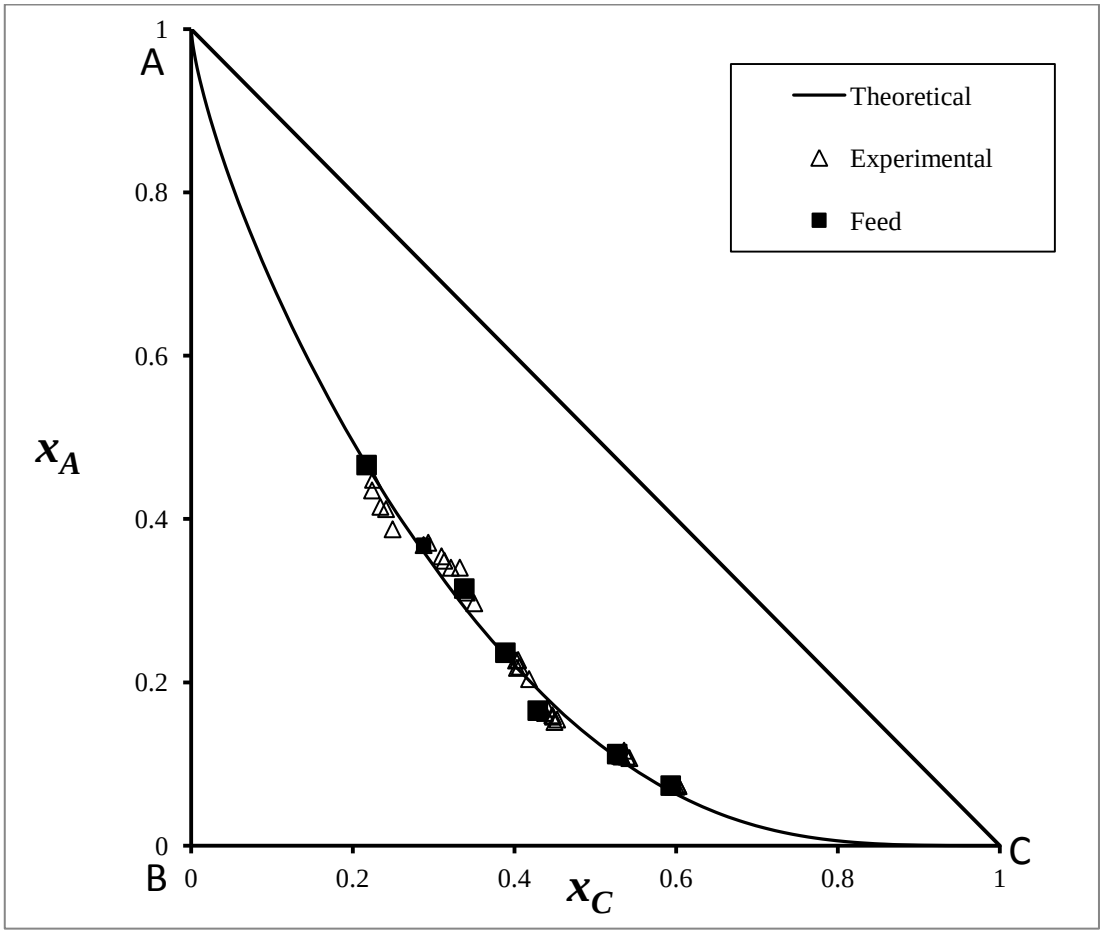

Figure 5.3: Experimental data for multiple different feeds on a single theoretical residue curve.

5.2 Stationary points behavioural results and discussion

For the evaluation of experimental stationary points effects on M-RCM behaviour, a point was taken close to pure hydrogen (the unstable node), a point close to pure carbon dioxide (the stable node), and a point close to pure carbon monoxide (the saddle point). These feeds and associated experimental data are represented in Figures 5.4 to 5.8.

5.2.1 Unstable Node behaviour

The experimental results obtained from the evaluation of the profile in the vicinity of the unstable node (hydrogen, point A) are depicted in Figure 5.4. It can be seen that the experimental data fits the theoretical data with a high accuracy and minimal deviations. The data produced is over a larger range in comparison to the other data since separations are usually easier at points close to the unstable node. This trend is due to the fast permeation of the large quantity of hydrogen close to the unstable node.

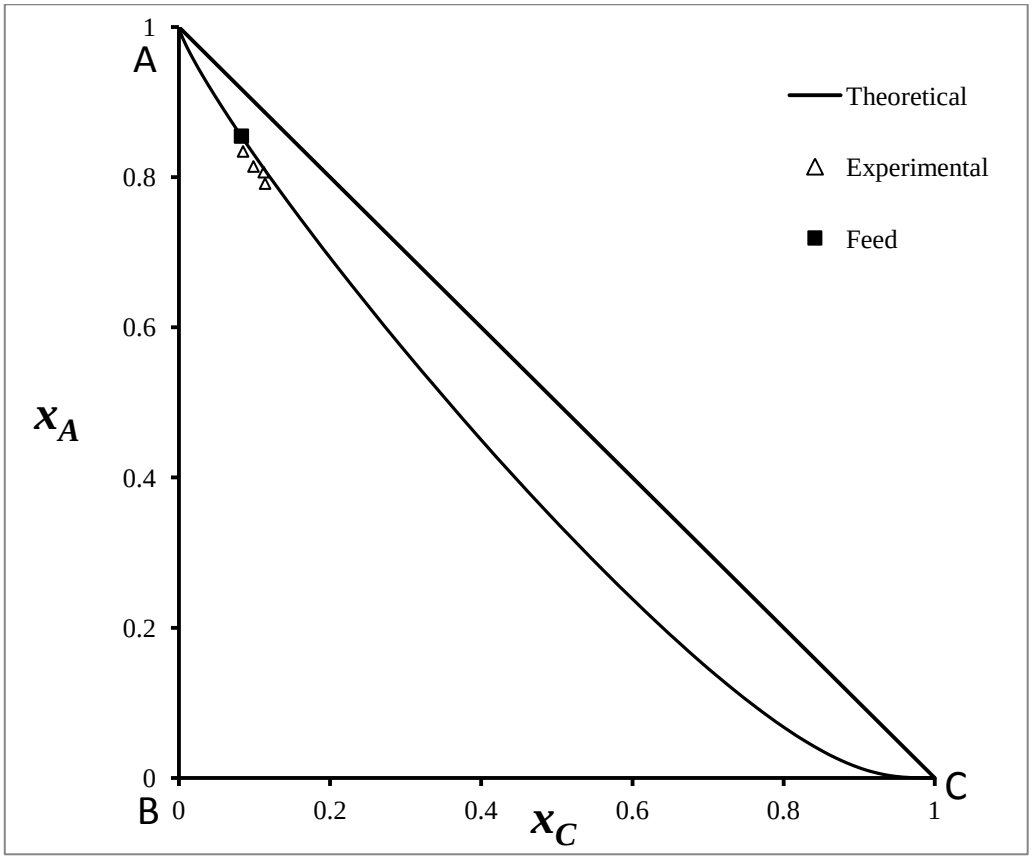

Figure 5.4: Experimental data behaviour in the vicinity of the unstable (H_2) stationary point.

5.2.2 Stable Node behaviour

The experimental data in the region of the stable node, carbon dioxide (point C), is represented in Figure 5.5, and a zoomed in version is given in Figure 5.6.

It is worth mentioning that in this particular case (where the feed location was close to pure carbon dioxide), the data points do not move sequentially towards the stable node. This phenomenon has no significance to the experimental procedure or apparatus employed, but rather can be attributed by the possible error in the gas chromatography detection. During the membrane separations the change in the retentate composition is fairly small, as can be seen from Figures 5.5 and 5.6. Composition detectors such as gas chromatographers find difficulty in detecting such small change hence the cause of the above mentioned phenomena. There could possibly be a form of error in the sampling of the retentate due to the degree of agitation in the retentate which could also result in this phenomenon. However, the bulk of the experimental data obtained fit the theoretical data with minimal or no deviations.

With that said, it can be deduced that the data fits theory with good accuracy. The data is produced close to the stable node since all data will move towards pure carbon dioxide. This is expected as according to theory carbon dioxide permeates the slowest, remaining in the retentate.

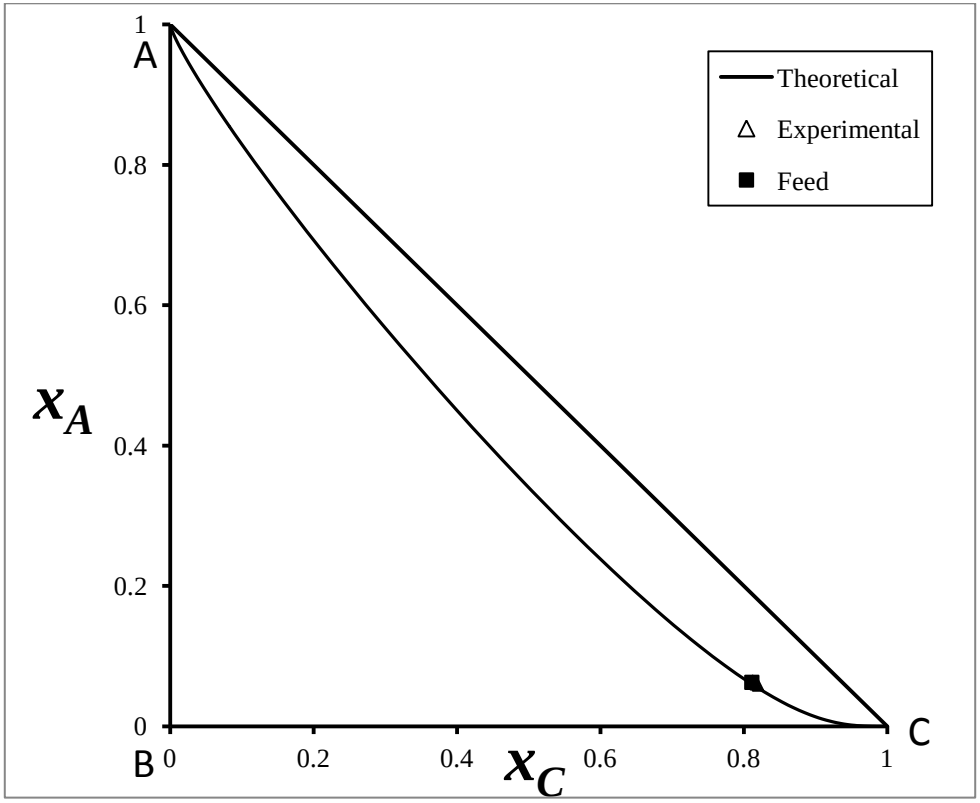

Figure 5.5: Behaviour of the experimental data in the vicinity of the stable (CO_2) stationary point.

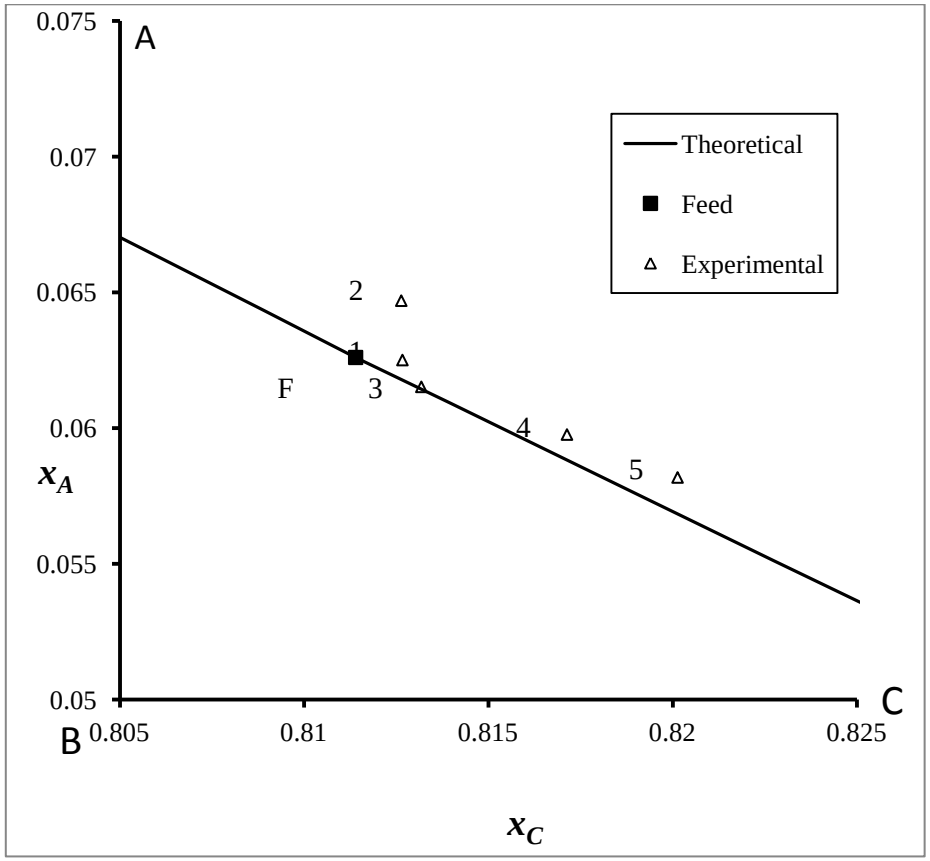

Figure 5.6: Zoomed in representation of experimental and theoretical data in the vicinity of the stable node, carbon dioxide. The order of the samples were taken are indicated numerical.

5.2.3 Saddle Node behaviour

Figure 5.7 depicts the experimental data obtained for different feed points on the same theoretical residue curve near the saddle node. The component near the saddle node has an intermediate permeation rate (between the components of the stable and unstable node) thus separation is difficult hence resulting in high curvature. The analysis of a residue curve near the saddle point is thus important as it has been predicted difficult to reproduce experimental data around the curvature of residue curves with minimal deviations.

As seen in Figures 5.7 and 5.8 the data around the curvature produces very small ranges, although the data still fits the predicted trend and the points do move towards the stable node thus reproducing the curvature. The predicted large deviation from theoretical data did not occur and the data produced around the curvature fits the trend with small errors. In accordance with Figures 5.7 and 5.8 the errors obtained in the saddle region are greater than the other regions analysed due to the increased difficulty of separation in this region.

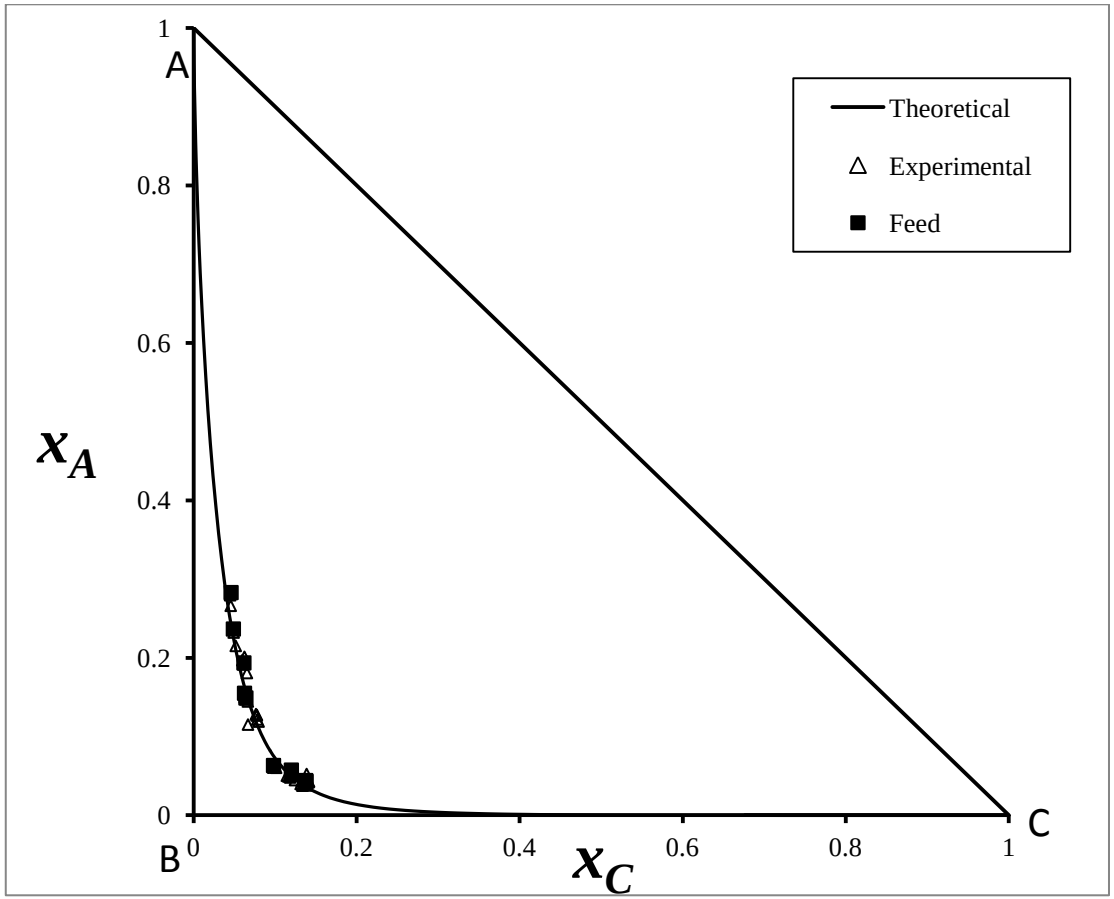

Figure 5.7: Experimental data behaviour for different feed points on the saddle node (CO).

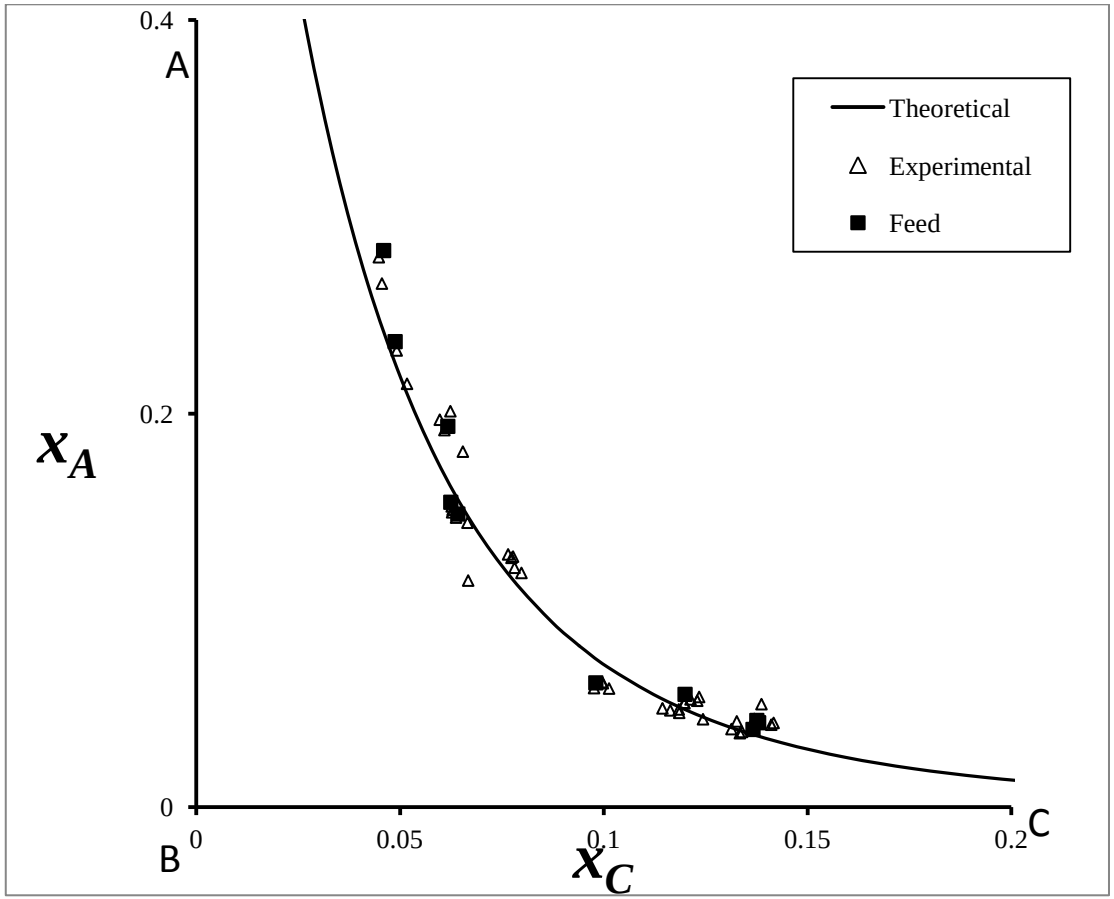

Figure 5.8: Zoomed in representation of the experimental data for the saddle node depicted in Figure 5.7.

The accuracy of experimental data against theoretical data proves the validation of the concept of M-RCM and its applications thereof. This also implies that the experimental set up and procedure were successfully designed and operated. Furthermore this accuracy validates the assumption of a basic flux model in the predication of experimental data and more importantly validates the use of residue curve maps in the design and optimisation of membrane separation processes.

5.3 Experimental error analysis

Apart from small deviations in the data represented in the Figures of Chapter 5, the data fits theory with a good accuracy. The data that did result in relatively large deviation are accounted for by the following possible experimental errors:

- Uncontrollable and undetectable leaks;
- Leaks within the system through micro-punctures in the membrane;
- The system was not at complete vacuum conditions;
- The sample gas permeated through the apparatus;
- The permeability co-efficient changed with the change in partial pressure of the retentate;
- The errors produced by the gas chromatography effected results since the change in composition with time was small;
- The agitation by the small computer fans was not adequate for mixing purposes hence samples taken were not completely true to the retentate.

These errors were not quantified since the occurrence of the possible errors could not be controlled. Although these errors could have occurred, they can be considered to be miniscule since the results produced fitted the theory effectively

Chapter 6

Conclusion

Membrane separation process design is becoming an important point of research and is increasingly required for applications in industry as membrane and hybrid membrane-distillation system are becoming more widely applied. There is very limited research on the topic of effective membrane design tools in the chemical engineering field. The use of M-RCMs has proved that it could be a very useful and effective graphical tool in the design of membrane and hybrid systems as residue curve mapping has been widely adopted in industry to design simple and complex distillation processes.

An experimental set up was successfully designed and operated for the measurement of M-RCMs. For the purposes of demonstrating the method, a relatively simple separation was employed. This was done by separating a gas mixture consisting of synthesis gas (carbon dioxide and hydrogen) and a carbon dioxide impurity through a polyethylene membrane. Four different regions were chosen for discussion namely the three stationary points and a single curve in the middle of the residue curve map. All of the data points obtained in each region tend toward the stable node (carbon dioxide) in accordance with theory that indicates carbon dioxide is the slowest permeating species in the gas mixture.

The bulk of the experimental data obtained fit the theoretical data with a high level of accuracy, although possible causes of error have been mentioned. The data produced at pure hydrogen, the unstable node, is over a larger range in comparison to the other data since separations are usually easier at points close to the unstable node. Data points closer to the stable (carbon dioxide) node correlate to theory as carbon dioxide, which permeates the slowest, remains in the retentate. Data at the saddle point (carbon monoxide) shows that deviations increase from theory as the data points move closer to curvature. This trend is best explained by the difficulty of separation associated with saddle point behaviour therefore predictions of data around this point are associated with a certain level of error tolerance.

This dissertation provides substantial data that correlate to the theoretical models and therefore it can be concluded that M-RCMs have been validated, and that the initial proposals put forward by Peters et al. (2006) regarding the nature and behaviour of these maps is verified. In addition, the experimental apparatus designed can be used for the validation of M-RCMs for any type of membrane and mixture of gases.

Recommendation

With this initial validation in place, future experimentation can use this dissertation to research the behaviour of more complicated gas mixtures through different types of membranes.

The experimental set up can also be used to determine whether inexpensive non-selective membranes such as the one used in this work can be used as an alternative to very expensive selective membranes in the separation of gases. Experiments can be run with a certain composition of gases being permeated through both a selective and non-selective membrane. Through determining the number of non-selective membranes required and hence the total area required, the costs associated with the process can also be determined. Comparing the capital and operating costs of the non- selective process in comparison to the selective membranes (capital intensive and very expensive to replace) it can be determined whether using a non-selective would be more economical and efficient.

References

Brubaker, D.W. & Kammermeyer, K., **1953.** Flow of gases through plastic membranes. *Ind. Eng. Chem*. 45, pp.1148-1152.

Doherty, M. F. & Malone, M. F., **2001**. Conceptual Design of Distillation Systems. *McGraw-Hill*: New York.

El-Bourawi, M.S., Ding, Z., Ma, R. & Khayet, M., **2006.** A framework for better understanding membrane distillation separation process. Member. Sci, *285*, pp. 4-29.

Fien, G. A. F. & Liu, Y. A., **1994**. Heuristic Synthesis and Shortcut Design of Separation Processes Using Residue Curve Maps: A Review. *Ind. Eng. Chem. Re*, 33, pp. 2505-2522.

Geankoplis, C.J., **1993**. Transport Processes and Unit Operations. 3rd ed. *Prentice-Hall, Inc*: New Jersey, pp. 760

Lawson, K. W. & Lloyd, D.R., **1997.** Membrane distillation. *Membrane. Sci, 124.* pp. 1-25.

Mason, E.A. & Kronstadt, B., **1967.** Graham's Law of Diffusion and Effusion. *Journal of Chemical Education*, Vol. 44, pp. 740-744.

Michaels, A.S. & Bixler, H.J., **1961**. Flow of Gases Through Polyethylene. *Journal of Polymer Science.* L, pp. 413-439.

Hinchliffe, A.B. & Porter, K.E., **2000.** A comparison of membrane separation and distillation. *Trans IChemE*, 7, pp. 255-269.

Pandey, P. & Chauhan, R.S., **2001.** Membranes for gas separation. *Prog. Polym. Sci*, 26, pp. 853-893.

Peters, M., Kauchali, S., Hildebrandt, D. & Glasser D., **2006**. Derivation and Properties of Membrane Residue Curves. *Ind. Eng. Chem. Res*, 45, pp. 9080-9087.

Peters, M., Kauchali, S., Hildebrandt, D. & Glasser D. **2008**., Application of Membrane Residue Curve Maps to Batch and Continuous Processes. *Ind. Eng. Chem. Res,* 47, pp. 2361-2376.

Pettersen, T. & Lien, K.M., **1995**. Design studies of membrane permeator processes for gas separation. *Gas. Sep. Purif*, 3, pp. 151-169.

Rautenbach, R. & Albrecht, R., **1989**. Membrane Processes. *John Wiley*: New York.

Sheffield Hallam University, **(n.d.).** *Gas Chromatography.* [Online]. Accessed from: http://teaching.shu.ac.uk/hwb/chemistry/tutorials/chrom/gaschrm.htm [Date Accessed: 26/05/2011]

Stephan, W.; Nobel, R.D.; Koval, C.A., **1995**. Design methodology for a membrane/ distillation column hybrid process. *J. Membr. Sci, 99*, pp. 259-272.

Wijmans, J. G. & Baker, R. W., **1995**. The solution-diffusion model: a review. *J. Membr. Sci*, 107, pp. 1-21.

Appendix A: Derivation of the Residue Curve Equation

Refer to Figure 3.1. Equation (3.2) can be expanded using the well-known chain-rule:

$$0 = \dot{P}.y_i + \frac{d}{dt}(R\,.x_i) = \dot{P}.y_i + R\,.\frac{d}{dt}\,(x_i) + x_i.\frac{d}{dt}(R)$$

Substituting in equation (3.1):

$$0 = y_i \cdot\left(-\frac{d}{dt}(R)\right) + R\cdot\frac{d}{dt}(x_i) + x_i\cdot\frac{d}{dt}(R)$$

Rearranging:

$$\frac{R\dfrac{d}{dt}(x_i)}{-\dfrac{d}{dt}(R)} = (x_i - y_i)$$

And cancelling:

$$-R\frac{d}{dR}(x_i) = (x_i - y_i)$$

Now, it can be shown that:

$$\frac{d}{dR}\left(\ln\left(\frac{k}{R}\right)\right) = -\frac{1}{R}$$

Where *k i*s a constant. Hence:

$$d\ln\left(\frac{k}{R}\right) = -\frac{dR}{R}$$

Let:

$$d\tau = -\frac{dR}{R} \qquad ...(*)$$

Thus:

$$\frac{d}{d\tau}(x_i) = (x_i - y_i)$$

This is the residue curve equation, as given in Equation (4). Further manipulation is needed to define τ. By rearranging Equation (1) and substituting into (*):

$$d\tau = \frac{P}{R} dt$$

Or:

$$\tau = \frac{P}{R} t$$

Thus, at $t = 0$, $\tau = 0$, and $R = R(0)$, hence:

$$\ln\left(\frac{k}{Ro}\right) = 0$$

Or:

$$k = Ro$$

Thus:

$$d\tau = d \ln\left(\frac{Ro}{Rt}\right)$$

Or:

$$\tau = \ln\left(\frac{Ro}{Rt}\right) \text{ as discussed}$$

Appendix B: Experimental Results

Table B-1: Unstable Stationary Point (H_2) Experimental Data

Run	Sample	H_2	CO	CO_2
1	Feed	0.854560	0.062748	0.082692
	1	0.834201	0.080955	0.084844
	2	0.791396	0.094627	0.113977
	3	0.814155	0.087236	0.098610
	4	0.806578	0.081249	0.112173

Table B-2: Stable Stationary Point (CO_2) Experimental Data

Run	Sample	H_2	CO	CO_2
1	Feed	0.062602	0.12599	0.811402
	1	0.064694	0.12266	0.812641
	2	0.062508	0.12482	0.812672
	3	0.061520	0.12529	0.813185
	4	0.059763	0.12310	0.817136
	5	0.058182	0.12168	0.820137

Table B-3: Saddle Point (CO) Experimental Data

Run	Sample	H_2	CO	CO_2	Run	Sample	H_2	CO	CO_2
1	Feed	0.082063	0.824026	0.093911	6	Feed	0.193529	0.744755	0.061717
	1	0.063196	0.838773	0.098031		1	0.201216	0.736433	0.062352
	2	0.063576	0.8369	0.099524		2	0.196909	0.743347	0.059745
	3	0.060542	0.841864	0.097595		3	0.191631	0.747487	0.060882
	4	0.060316	0.838401	0.101283		4	0.18068	0.753906	0.065413
	5	0.063048	0.837196	0.099755					
					7	Feed	0.236567	0.714638	0.048795
2	Feed	0.057357	0.822717	0.119926		1	0.232111	0.71871	0.049179
	1	0.056032	0.820583	0.123385		2	0.21515	0.733137	0.051713
	2	0.054808	0.823922	0.12127					
	3	0.054131	0.822952	0.122917	8	Feed	0.154957	0.782592	0.06245

	4	0.052377	0.808947	0.138676		1	0.152871	0.784458	0.062671
						2	0.151187	0.785918	0.062895
3	Feed	0.044104	0.818363	0.137533		3	0.149871	0.787355	0.062774
	1	0.043633	0.823749	0.132618		4	0.115186	0.818101	0.066714
	2	0.041937	0.816985	0.141078					
	3	0.042845	0.815494	0.141661	9	Feed	0.148973	0.786848	0.064179
	4	0.044876	0.818202	0.136922		1	0.147181	0.78908	0.063739
						2	0.144574	0.788885	0.066541
4	Feed	0.042937	0.819084	0.137979		3	0.12674	0.795921	0.077339
	1	0.050244	0.835375	0.114381		4	0.127343	0.794935	0.077722
	2	0.052798	0.827421	0.119781		5	0.121704	0.800207	0.07809
	3	0.044715	0.830955	0.124331		6	0.128472	0.795014	0.076514
	4	0.049708	0.83191	0.118382		7	0.119059	0.801158	0.079782

	5	0.053139	0.827158	0.119703					
	6	0.047979	0.833528	0.118493	10	Feed	0.282846	0.671182	0.045973
	7	0.049251	0.834444	0.116305		1	0.279483	0.67572	0.044796
						2	0.266088	0.688355	0.045556
5	Feed	0.039531	0.823867	0.136601					
	1	0.039715	0.82897	0.131315					
	2	0.038283	0.827802	0.133915					
	3	0.039987	0.82408	0.135933					
	4	0.037641	0.828989	0.13337					

Table B-4: Middle Region Curve Experimental Data

Run	Sample	H_2	CO	CO_2	Run	Sample	H_2	CO	CO_2
1	Feed	0.466045	0.316846	0.217109	4	Feed	0.236219	0.375001	0.38878
	1	0.448023	0.326908	0.225069		1	0.227265	0.368234	0.404501
	2	0.435007	0.34114	0.223853		2	0.21917	0.374357	0.406473

	3	0.414973	0.350869	0.234158		3	0.226697	0.371347	0.401956
	4	0.387383	0.363313	0.249304		4	0.217685	0.379227	0.403088
	5	0.412127	0.346692	0.241181		5	0.203924	0.378007	0.418069
2	Feed	0.368063	0.344284	0.287652	5	Feed	0.1653	0.405917	0.428784
	1	0.370886	0.335737	0.293377		1	0.162487	0.39973	0.437783
	2	0.34894	0.337753	0.313307		2	0.16797	0.391368	0.440662
	3	0.340333	0.338269	0.321398		3	0.159594	0.393573	0.446833
	4	0.354289	0.335933	0.309779		4	0.154417	0.392803	0.452781
	5	0.3404	0.327172	0.332428		5	0.15795	0.394343	0.447707
						6	0.151442	0.399088	0.44947
3	Feed	0.314788	0.347271	0.337941					
	1	0.314965	0.344927	0.340107	6	Feed	0.112053	0.360893	0.527054
	2	0.309891	0.349018	0.341091		1	0.109904	0.357672	0.532424
	3	0.296792	0.352916	0.350292		2	0.109107	0.358538	0.532355
						3	0.109046	0.351921	0.539033
						4	0.10719	0.350661	0.542149
						5	0.110182	0.359493	0.530325
						6	0.116252	0.348188	0.53556